DOI 10.1515/htmp-2012-0094 — High Temp. Mater. Proc. 2012; 31(4-5): 569–580

Jingxi Zhu*, Jinichiro Nakano, Tetsuya Kenneth Kaneko, Haoyuan Mu, James P. Bennett, Kyei-Sing Kwong, Peter Rozelle and Seetharaman Sridhar

Viscosity Determination of Molten Ash from Low-Grade US Coals

Abstract: In entrained slagging gasifiers, the fluidity of the molten ash is a critical factor for process control since it affects slag formation, the capture of inorganic constituents, refractory wear, and slag drainage along the gasification chamber walls. The use of western coal, or mixtures of eastern and western coals as gasifier feedstock, is likely to occur as western coals become available and technological issues that hinder their use are being resolved. In the present work, the viscosity of synthetic slags with ash chemistries simulating the western U.S. coals, was experimentally measured at a $Po_2 = 10^{-8}$ atm in the temperature range of 1773–1573 K (1500–1300 °C) using a rotating-bob viscometer. Alumina spindles and containment crucibles of both alumina and zirconia were used. Crystallization studies of this slag using a confocal scanning laser microscope found that a $(Mg,Fe)Al_2O_4$-based spinel precipitated at temperatures below 1723 K (1450 °C), and this agreed with FactSage equilibrium phase prediction. The same spinels were observed in the post-viscometry experiment slags when ZrO_2 crucibles were used and assumed to be in equilibrium with the slag at the higher temperatures. Zirconia dissolution resulted in a slight increase in the solid fraction present in slags at lower temperatures, compared to spinel fraction. Crystal precipitation changed the apparent activation energy and required a longer stabilization times for viscosity measurements. The viscosity results were used in predictive equations based on Veytsman and Einstein's models, with critical nucleation temperatures and the solid fraction calculated with FactSage. In the simulated eastern/western coal feedstock blends based on ash compositions, the fractions of the solid precipitates were also calculated using the thermodynamic program FactSage for each blend composition, and the plastic viscosity of each eastern/western coal slag blend was predicted using Veytsman's model and compared to available experimental data.

Keywords: coal gasifier, slag, viscosity, plastic viscosity, crystallization

PACS® (2010). 66.20.+d

***Corresponding author: Jingxi Zhu:** US Department of Energy, National Energy Technology Laboratory, 626 Cochrans Mill Road, Pittsburgh, PA 15236-0940, USA; Department of Materials Science and Engineering, Carnegie Mellon University, 5000 Forbes Ave., Pittsburgh, PA 15213, USA
E-mail: jingxiz@andrew.cmu.edu
Jinichiro Nakano: US Department of Energy, National Energy Technology Laboratory, 1450 Queen Avenue SW, Albany, OR 97321-2198, USA; URS Corp, P.O. Box 1959, Albany, OR 97321 USA
Tetsuya Kenneth Kaneko: US Department of Energy, National Energy Technology Laboratory, 626 Cochrans Mill Road, Pittsburgh, PA 15236-0940, USA; Department of Materials Science and Engineering, Carnegie Mellon University, 5000 Forbes Ave., Pittsburgh, PA 15213, USA
Haoyuan Mu: Department of Materials Science and Engineering, Carnegie Mellon University, 5000 Forbes Ave., Pittsburgh, PA 15213, USA
James P. Bennett: US Department of Energy, National Energy Technology Laboratory, 1450 Queen Avenue SW, Albany, OR 97321-2198, USA
Kyei-Sing Kwong: US Department of Energy, National Energy Technology Laboratory, 1450 Queen Avenue SW, Albany, OR 97321-2198, USA
Peter Rozelle: Office of Clean Energy Systems, US Department of Energy, FE-22/Germantown Building, 1000 Independence Ave. NW, Washington, DC 20585, USA
Seetharaman Sridhar: US Department of Energy, National Energy Technology Laboratory, 626 Cochrans Mill Road, Pittsburgh, PA 15236-0940, USA; Department of Materials Science and Engineering, Carnegie Mellon University, 5000 Forbes Ave., Pittsburgh, PA 15213, USA

1 Introduction

High-temperature slagging gasifiers have the potential to gasify carbon feedstock such as coal, petroleum byproducts, biomass, or mixtures of them. Mixed carbon feedstock would increase fuel flexibility and lower net CO_2 output and emissions. Gasifiers also have the potential for carbon capture and storage (CCS). In an integrated gasification combined cycle (IGCC) power system, potential pollutants can be converted into reusable byproducts, and excess heat used to generate power in a steam turbine.

Slagging gasifiers in the U.S. predominately use bituminous or sub-bituminous coals east of the Mississippi River. The Western United States has deposits of low-rank coal that account for a significant fraction of U.S. coal reserves. These western U.S. coals include sub-bituminous and lignite ranks that have lower BTU/lb values and high moisture compared to the eastern bituminous and sub-bituminous coals. With the demand for low-cost and reliable power, the potential usage of western coals has become more important in the United States. To enable gasification (or co-gasification) of western coals, difficulties caused by the inorganic constituents in the fuel feedstock need to be overcome. In a slagging/entrained-flow gasification system, the inorganic constituents typically liquefy under the gasification conditions of T = 1598 to 1873 K (1325 to 1600 °C), P = 2.07–6.89 MPa and $\log(P_{O2}) = -9$ to −7. [1] The liquefied ash coalesces and forms a slag, which, ideally, deposits on the refractory walls, flows to the bottom of the gasifier, and is removed as a tapped slag stream.

Not all of the nongaseous impurities resulting from gasification leave the system with the slag stream, with some becoming entrained within the syngas, forming fly ash, which can interact with downstream components of the gasifier. Furthermore, depending on the slag properties; it can either be too viscous, which can inhibit tapping from the gasifier, or too fluid, causing excessive degradation of the refractory liner. [1]

As such, maintaining optimum slag properties in a gasifier can require a balance between two extremes that on one hand can result in operations issues caused by poor slag flow, and on the other hand maintenance issues caused by excessive refractory degradation. Slag fluidity can be expected to be a function of system temperature and slag chemistry, which can to some degree be controlled in the system. However, a better fundamental understanding of slag properties under gasification conditions can result in improved control strategies in plant operations, especially in maintaining the optimum balance between slag flow and refractory wear. The composition, structure, and resulting properties of the slag are critical to the operation of the gasifier; improvements in these areas have the potential to enhance the commercial competitiveness of IGCC technology.

Slag viscosity depends on ash chemistry, temperature, oxygen partial pressure (determined by the CO/CO_2 ratio in the gasifier), and the precipitation of solid phases. Ash chemistry depends on the source of the coal and/or any additional carbonaceous feedstock it is mixed with, such as other types of coal or petcoke. For example, low-rank coal westerns U.S, compared to eastern US coal, [2] is significantly richer in CaO, which is a strong depolymerizing unit in silica based slags. Table 1 shows typical ash chemistries of coals in the United States.

Evaluations of molten coal-ash viscosity and semiempirical estimation models have been presented in the literature, [3–7] but the effect of crystallization has not been extensively and explicitly treated by these models, and would be a pertinent factor in the viscosity of alkali-rich western slags. The aim of this study is to evaluate and predict the viscosities of synthetic slags resembling the molten ash chemistry of eastern and western (west of the Mississippi river) coal slag mixtures, and to account for the solid fractions in the slag through Einstein's equation [8] used for dilute suspension, and Veytsman's model [9] that is used to predict slurry viscosities.

2 Experimental

2.1 Sample preparation

The compositions of the two synthetic slags chosen for viscosity and phase studies were from known fuel ash compositions of coal feedstock in the United States. The eastern coal (EC) slag was determined based on averages of coal chemistries in a report by Selvig and Gibson [10], where over 300 US coals were analyzed. Western coal (WC) slag chemistry was determined by averaging ash compositions of the Wyodak-Anderson and Beulah-Zap seams reported by Vorres. [11]

The two slags were synthesized by mixing the individual oxide components in powder form to the appropriated ratios, then pre-melted and equilibrated in a gas mixture of CO/CO_2 at 1773 K (1500 °C). The CO to CO_2 ratio was 1.8, corresponding to a $P_{O2} = 10^{-8}$ atm, at which 99.92 at% of the Fe ions should be 2+, the balance being 3+, as determined with FactSage thermodynamics software. [7] The dissolution of the Al_2O_3 crucible used to contain the molten slags during pre-melting was minor for eastern coal slag, but was substantial for the western coal slag, resulting in almost a 5 wt% increase in Al_2O_3 content. The target slag compositions and the slag compositions after melting (labeled with "VS") are listed in Table 2, as well as the compositions after viscosity measurement. The slag compositions were evaluated using X-ray fluorescence (XRF) spectrometry. Eastern coal slags are labeled with "EC" and western coal slags with "WC". A typical post-measurement slag composition (EC-post) is shown for eastern coal slag. "M" stands for "viscosity measurement" and is followed by the viscosity measurement

a)

Seam*	State	C	H	O	S	Ash
Illinois No. 6	IL	78	5	14	4.8	15
Pittsburgh (No. 8)	PA	83	5.3	9	2.2	9
Wyodak-Anderson	WY	75	5.4	18	0.6	9
Beulah-Zap	ND	73	4.8	20	0.8	10

* Illinois No 6 and Pittsburgh (No 8) are examples of Eastern coals used for gasifiers, and Wyodak and Beulah are examples of Western coals

b)

	Illinois No. 6	Pittsburgh (No. 8)	Beulah-Zap	Wyodak-Anderson
Al_2O_3	18.3	25.2	10.22	15.5
BaO	0.02	0.84	–	0.5
CaO	7.9	2.6	24.72	15.1
Fe_2O_3	18	19.5	8	10.2
K_2O	2.9	2.1	0.94	0.8
MgO	1.2	1.3	7.48	3.6
MnO	0.04*	0.14*	–	0.04
Na_2O	0	0	7.76	1.5
P_2O_5	0.2	0	0.48	1.2
SO_3	6.8	2	17.55	22
SiO_2	43.7	45.9	18.4	28.7
SrO	0.05	1.12	–	0.4
TiO_2	1	1.2	0.48	1.2
Undetermined	–	–	–	1.87

* = Mn_3O_4

Table 1: Examples of several different U.S. coal chemistries based on geographic location. a) overall composition, and b) ash chemistry in weight percentage [2]

a)

wt%	Al_2O_3	CaO	Fe_2O_3	K_2O	MgO	MnO	Na_2O	P_2O_5	SiO_2	TiO_2	ZrO_2
Target [11]	26.50	6.10	17.90	1.50	1.30	0	0.90		45.80		
EC-VS	26.05	6.55	18.44	2.24	1.28	0.042	0.75	0.022	44.52	0.067	0.035
EC-post	26.09	6.53	18.29	2.23	1.29	0.044	0.82	0.027	44.38	0.067	0.23

b)

wt%	Al_2O_3	CaO	Fe_2O_3	K_2O	MgO	MnO	Na_2O	P_2O_5	SiO_2	TiO_2	ZrO_2
Target [11]	16.88	25.97	11.89	1.10	7.29		5.99		30.87		
WC-VS	21.69	25.77	10.53	1.41	6.05	0.098	5.25	0.017	28.87	0.033	0.07
WC-M1	31.12	22.50	9.30	1.19	5.42	0.086	4.58	0.016	25.49	0.036	0.004
WC-M2	23.21	20.90	8.41	1.13	5.28	0.086	4.20	0.039	26.83	0.037	9.64
WC-M3	22.87	23.24	8.46	1.22	5.50	0.096	4.76	0.030	26.89	0.047	6.66

Table 2: Composition of the experimental slags from: a) eastern coal b) western coal

number. Note that the ZrO_2 pick-up from crucibles was substantial for WC-M2 and WC-M3. Alumina spindles were used in all viscosity measurements, and the crucible materials and atmospheres used during viscosity testing is shown in Table 3.

2.2 Viscosity measurements

The viscosity measurements were carried out using the rotating cylinder method described in ref. [12] and shown in Figure 2a. The core component of the viscometer is the

Measurement No.	Crucible	Atmosphere	P_{O2}	Data collection method
WC-M1	Al_2O_3	CO/CO_2	10^{-8} atm	Manual
WC-M2	ZrO_2	CO/CO_2	10^{-8} atm	Auto
WC-M3	ZrO_2	CO/CO_2	10^{-8} atm	Auto

Table 3: The crucible materials and atmospheres used in the viscosity measurements

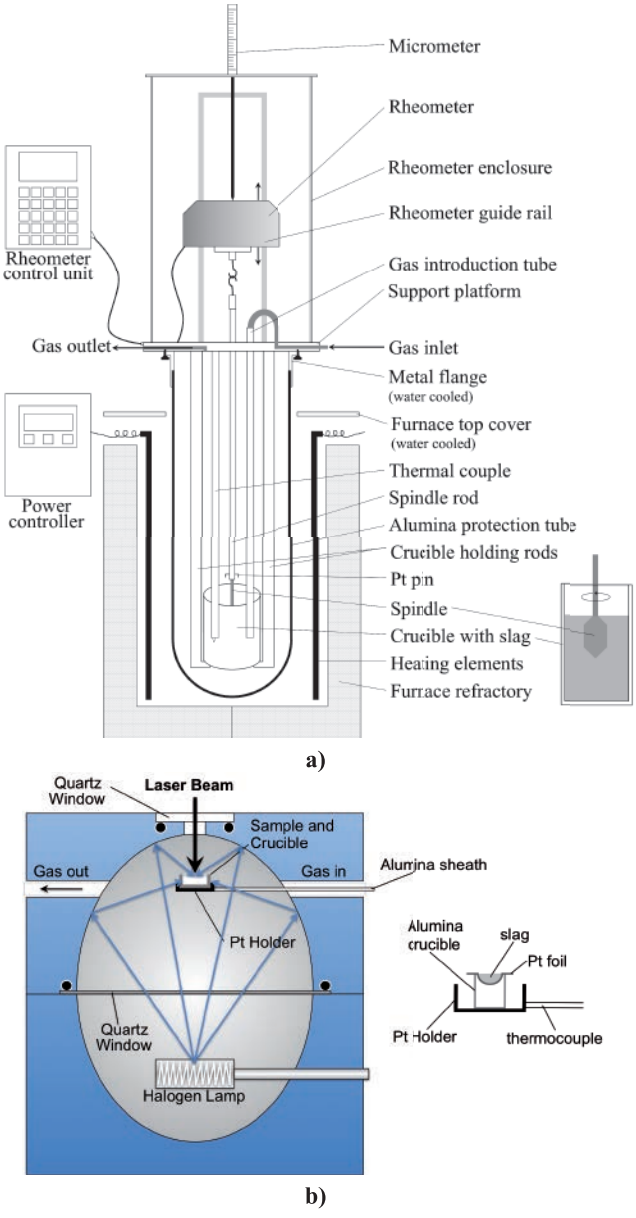

Fig. 1: (a) Schematic of viscometer and (b) schematic of CSLM.

Brookfield Rheometer (model DV-III) that controls the rotation speed of the spindle and converts the torque exerted on the spindle head into a viscosity reading. The heating of the furnace is controlled by the readings from the thermocouple placed beside the crucible filled with slag. The viscometer was calibrated at 298 ± 0.1 K before each measurement using three oil standards with viscosities of 4.95 Pa·s, 12.16 Pa·s and 58.56 Pa·s.

The viscosity of the slags were measured in a step-cooling cycle of 25 K increments (1773–1573 K), with a thermal equilibration time at each temperature of 30 min before measurements were taken. A continuous flow of the CO/CO_2 gas was maintained at a flow rate of 0.2 ± 0.01 l/min during each experimental run. The viscosity data was recorded in two ways, one by manually adjusting the spindle rotation speed at each temperature so that the torque was between 70–80% of the full torque, with the viscosity reading averaged within the oscillating range of the torque reading that is less than ±0.3%. The other way was using a dedicated computer software package to control the rheometer and to record the viscosity reading at the same time. The range of the torque was pre-set to 70–80% for obtaining viscosity readings. After the 30 minutes of thermal equilibration time, the viscosity was recorded for another 30 minutes (referred to as data acquisition time). The time of data recording was reduced for 1773 K (1500 °C) and 1748 K (1475 °C), since the slag stabilized faster at high temperatures. In the computer-operated data collection, viscosity values were recorded every 3 seconds. A single viscosity value for each temperature was obtained by averaging all the viscosity readings recorded in data acquisition time at each temperature.

After the viscosity had been measured at the lowest temperature, i.e. 1573 K (1300 °C), the spindle was lifted out of the slag, and the slag was then cooled to room temperature by turning off the furnace. The slag composition was routinely analyzed by XRF and XRD before and after each measurement. The slag, slag/crucible and slag/spindle interfaces were also characterized with SEM.

2.3 Crystallization of western coal slag

In order to assess the crystallization tendency of the western coal slag, a confocal scanning laser microscope

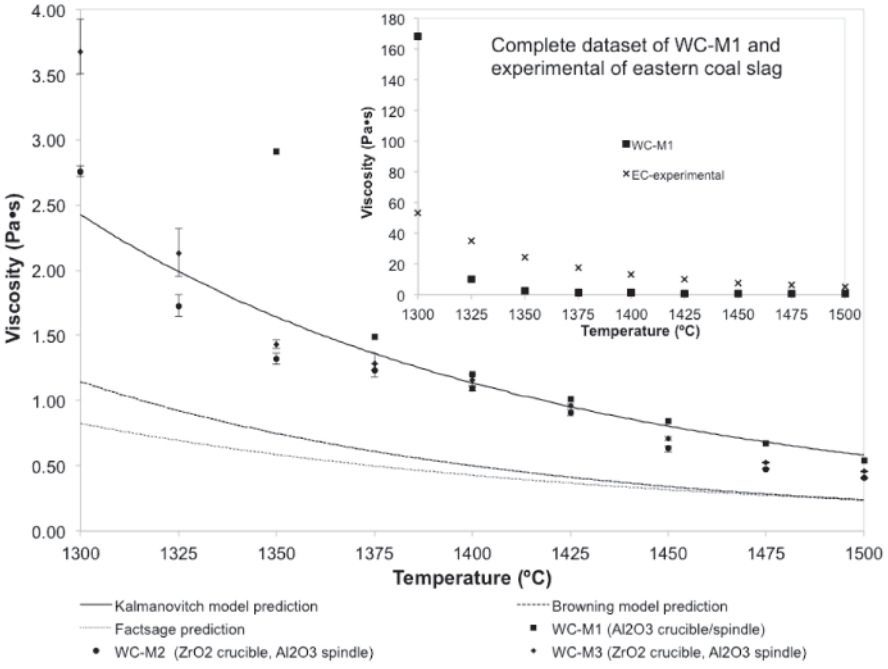

(a)

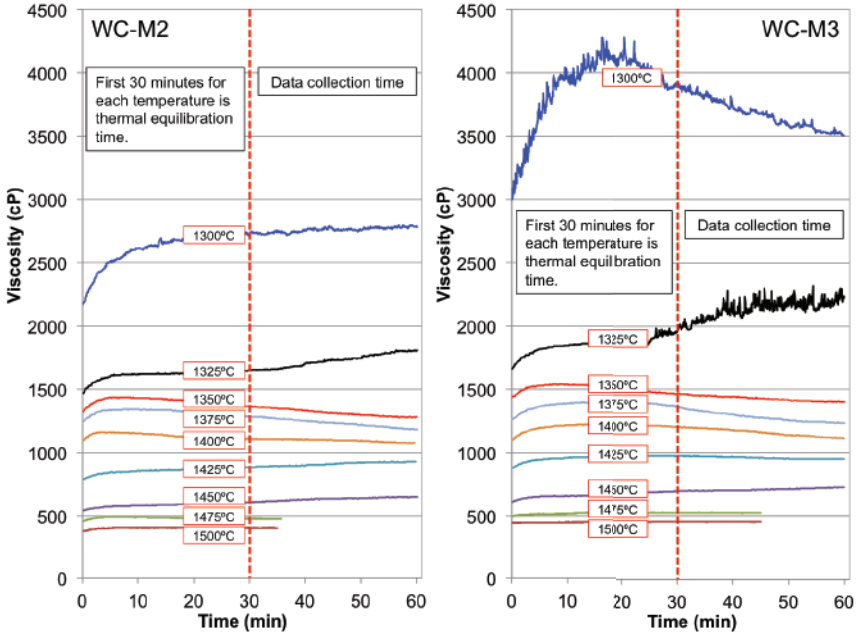

(b)

Fig. 2: (a) Measured viscosity vs. temperature and (b) Measured viscosity vs. time at the various temperatures.

(CSLM) was used for the study of the crystallization that had a gold image hot stage attached to the microscope, see Figure 1b. This system has fast heating and cooling capabilities. Details of the CSLM have been documented in literatures, [13–16] but the key features of the system are (i) confocal optics with a source of He-Ne laser (wavelength of 632.8 nm) allowing for imaging of features in a narrow focal plane while filtering background glare due to radiation and (ii) an infra red heating system which allows for rapid heating and cooling. Using this system, crystal precipitation in semi-transparent slags or on the surface of opaque slags could be observed in-situ.

In each experiment, approximately 0.010~0.020 g of starting slag powder was poured into a bowl made from platinum foil (99.99%, 0.05 mm thick), which was then placed onto an Al_2O_3 crucible. The crucible with slag were set on a platinum sampler pan and placed into the hot stage, see Figure 1b. Each starting slag powder in the Pt bowl was heated in the CSLM hot stage in a CO/CO_2 gas ratio of 1.8. In order to start from a completely molten slag, the slag powder was heated to 1823 K (1550 °C) and held for 10 minutes. The slag was then rapidly cooled (approximately 100 °C/s) to the desired crystallization temperature, typically in a few seconds, and held isothermally for another 10 minutes. The slag crystallization event was optically observed and recorded in situ, and the time needed for the precipitation to occur on the surface of the slag liquid was recorded for each temperature. After crystallization had occurred at each crystallization temperature, the slags were quenched to room temperature to evaluate the crystallized phases using the SEM and XRD.

3 Results and discussions

The measured viscosity vs. temperature for the western coal composition are shown in Figure 2a, and the maximum and minimum viscosities recorded in the data acquisition time at each temperature are shown as the error bars. It can be seen, when compared to the measured viscosity of eastern coal ash under similar conditions, [12] also shown in Figure 2a as "EC-experimental", the viscosity of western coal slag is generally an order of magnitude lower. Furthermore, viscosity of western coal does not appear to be a continuous function but instead exhibits at least two distinct changes in curvature. Of the viscosity models evaluated, the experimental results agreed most with the Kalmanovitch and least with the Browning predictions. The Kalmanovitch model considers a spectrum of experimental data, including those containing crystalline solids, and fits the slag system with respect to a Weymann-Frenkel relationship. Accordingly, the Kalmanovitch model predicts slag viscosities that contain fugitive solids. On the other hand, the Browning model is not as adaptable in predicting viscosities for slags that are outside the Newtonian region, such as when a crystalline phase precipitates in a slag. The Browning model is based on the assumption that the viscosity-temperature curve is identical for all coal slags (in the Newtonian region), and thus a standard curve is shifted along the temperature axis based on composition.

Figure 2b shows the change in viscosity during isothermal holds at each temperature for two measurements:

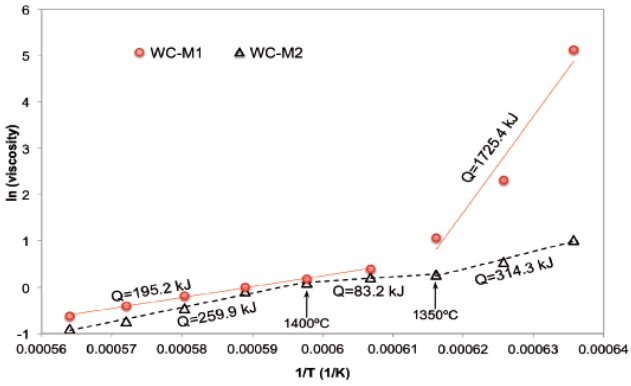

Fig. 3: Natural logarithm of viscosity vs. inverse of temperature for two of the measurements, where *Q* is the activation energy. The third measurement (WC-M3) was nearly identical to WC-M2.

WC-M2 and WC-M3. It is seen that below 1673 K (1400 °C), there was a measurable viscosity change with time, indicating some dynamic change in the slag. Figure 3 shows the natural logarithm of the measured viscosity vs. the inverse of temperature, and if an Arrhenius type temperature dependency were to hold, then the slope(s) of the plot would be proportional to the activation energy for viscous flow. It is clear from the plot that single activation energy does not describe this system. The activation energy corresponding to the high temperature range is within the values found in eastern coals. [12]

The drastic and discontinuous changes in the measured viscosity could be an indication of a phase change occurring in the slag, and that the gradual increase in the slopes of the viscosity vs time curves at the lower temperatures in Figure 2a is an indication that this phase change is occurring within the time scale of the measurement at the lower temperatures. Above 1350 °C, however, the relatively stable viscosity values with time suggest that the phase change was rapid, and was completed within the 30-minute equilibration time, thus probably not impacting viscosity measurements. The most likely physical change that this slag would undergo is crystallization.

In the western coal slag viscosity measurement taken using an Al_2O_3 crucible, dissolution of the crucible material resulted in extensive slag crystallization, shown in Figure 4a, compared to measurements taken with ZrO_2 crucible. A large amount of so called "CAS" phases precipitated, which were made up of CaO, Al_2O_3 and SiO_2 with certain ratios. Therefore, the WC-M1 dataset was deemed not suitable for further use in plastic viscosity prediction. ZrO_2 crucible was also attacked by the slag, however, the dissolution of ZrO_2 did not seem to affect the precipitation of crystalline phase, Figure 4b. ZrO_2 dissolved into the slag at high temperatures and precipitated as dendrites at low

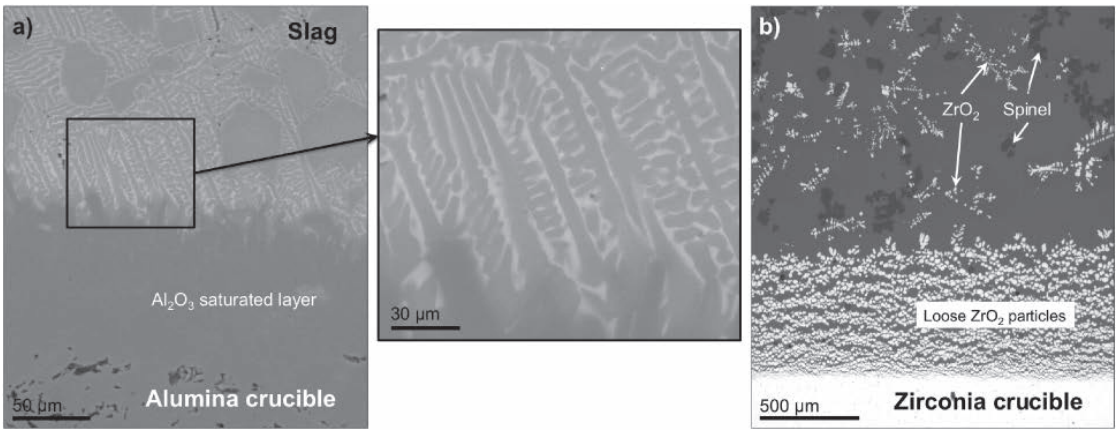

Fig. 4: Micrographs of slag/crucible interface for a) WC-M1 and b) WC-M2.

temperatures and did not seem to have combined with any oxide component from the slag.

Figure 5 shows the FactSage prediction of the weight percentages of the solids in the slag, with and without ZrO_2 dissolution. The FactSage calculations were conducted using major components (Al_2O_3, CaO, Fe_2O_3, MgO, Na_2O, SiO_2 and ZrO_2) taken from Table 2 with $Po_2 = 10^{-8}$ atm. For the calculation to simulate the case with no ZrO_2 content in slag, the compositions in Table 2 were normalized with ZrO_2 removed from the slag composition. The ZrO_2 solid phase was considered to be a solution phase rather than a stoichiometric compound throughout the calculations. Then, the volume fractions in the two cases were calculated by estimating the density of the liquid slag as a function of chemistry using the method described in ref. [16]. The densities of spinel and ZrO_2 were taken as constants and were 3.64 g/cm^3 [17] and 5.68 g/cm^3 [18], respectively.

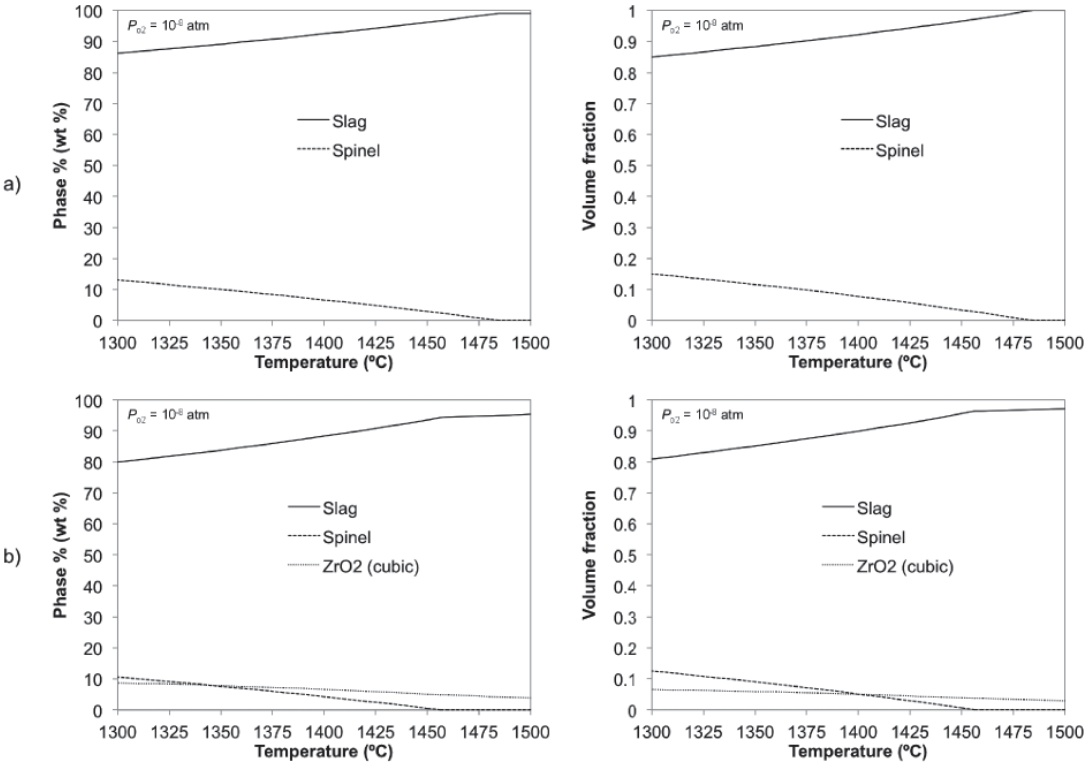

Fig. 5: Phase percentage vs. temperature (a) without ZrO_2 (b) with ZrO_2 at $Po_2 = 10^{-8}$ atm.

T-ranges where new crystal forms	Crystals (phases) found in FactSage		Crystals (phases) found experimentally	
	with ZrO_2	without ZrO_2	in quenched slag after viscometry	in slags at the TTT study in Pt-CSLM
1500	ZrO_2			spinel
1484.45*	ZrO_2	spinel		spinel
1475	ZrO_2	spinel		spinel
1456.23*	ZrO_2 and spinel	spinel		spinel
1450	ZrO_2 and spinel	spinel		spinel
1425	ZrO_2 and spinel	spinel		spinel
1400	ZrO_2 and spinel	spinel		spinel
1375	ZrO_2 and spinel	spinel		spinel
1350	ZrO_2 and spinel	spinel		spinel
1325	ZrO_2 and spinel	spinel		spinel
1300	ZrO_2 and spinel	spinel	ZrO_2 and spinel	spinel

* Transition temperatures indicated by FactSage.

Table 4: Solid phases thermodynamically predicted by Factsage and found experimentally in the western coal slag

It is seen that the solid volume fraction predicted without ZrO_2 is in the range of 0–0.15 (the faction is based on 1.00 being 100 pct solid), and that introducing ZrO_2 to the slag by dissolution of the crucible resulted in a slight delay in the precipitation of spinel, and that it dissolved into the slag at elevated temperatures.

Table 4 compares the expected solid phases predicted by FactSage with and without ZrO_2 present and compares those to what was found in two experimental cases. The reason that the amount of ZrO_2 predicted to be present in the slag was being determined was to evaluate its influence on viscosity values measured. In the first case (column 4), the phases listed were found after the viscosity measurements were taken, i.e. ZrO_2 and spinel. It should be noted that these slags were not quenched, and therefore a distinction cannot be made whether crystallization observed occurred at the experimental temperature or during cooling. Nevertheless, it can be seen that the crystalline phases found in the spent slag agrees with the FactSage prediction when ZrO_2 is taken into account. The last column to the right lists the crystals that were observed in-situ in the CSLM in a Pt crucible during isothermal holds after they were allowed to grow. The spinel phase is the primary phase predicted and observed in samples, and it precipitates whether ZrO_2 is or is not present. The spinel phase is $(Mg,Fe)Al_2O_4$ was found in both the viscometry slag and CSLM slag of the western coal, with some solid solutions of Mg^{2+} and Fe^{2+}. As seen in Figure 4b, the size of the spinel in the viscometry slag ranges from 50 to 200 μm.

To incorporate the effect of solid fraction and predict the plastic viscosity, two models from the literature were considered; the model proposed by Veytsman for predicting slurry viscosities [9], and Einstein's equation (see e.g. ref. [8]).

Einstein's equation is given below. It adjusts the clear liquid viscosity, η_0, with the solid volume fraction, ϕ. Einstein's equation considers spherical particles when $\phi \ll 1$ but does not consider any particular particle size distribution.

$$\eta = \eta_0\left(1+\frac{5}{2}\phi\right), \tag{1}$$

where η is the effective viscosity, η_0 is the clear liquid viscosity, and ϕ is the volume fraction of the solids. The Veytsman's model [9] is shown below,

$$\eta = \eta_0\left(1-\frac{\phi}{\phi_{\max}}\right)^{-[\eta]\phi_{\max}} \tag{2}$$

where $[\eta]$ is the intrinsic viscosity, and $\phi_{\max}$ is the solid fraction when the close packing limit is reached.

Using the Einstein equation as a starting point, the Veytsman model adds the influence of the particle size distribution of the fugitive solids on the clear liquid viscosity. The model parameterized this aspect of the system by means of examining the ratio between a given solid fraction (ϕ) and the maximum solid fraction ($\phi_{\max}$) possible for this system. For any given composition $v_1, v_2, \ldots, v_n$ of a blend with particle sizes $D_1, D_2, \ldots, D_n$; $\phi_{\max}$ is calculated using an iterative algorithm (see ref. [9] for details). For spherical particles of a single size, $\phi_{\max} \approx 0.637$. The value of $\phi_{\max}$ changes, however, with the size distribution and shape of the particles in the slag. For simplicity, spherical particles (shape factor = 1) are assumed in this

study with a close pack ratio (ϕ_0) of 0.637. It should be mentioned, though, that shape factor is factored into the close pack ratio (ϕ_0), and can have a significant effect on the plastic viscosity by changing the value of ϕ_{max}, even at low solid volume fraction regime. In the $0 < \phi < 0.2$ solid volume range considered here, the value of ϕ_{max} resulted from a shape factor close to unity is much larger than ϕ. However, if a small shape factor is used, say 0.2, the maximum solid loading (ϕ_{max}) may decrease to a similar magnitude as the actual solid loading (ϕ). Although the particle size distribution can only change the value of ϕ_{max} in a small range, regardless of the shape factor, it can be proven mathematically that the plastic viscosity is sensitive to even a small change of ϕ_{max} when ϕ_{max} is close to the ϕ.

Experimental data indicate that the value for [η] only changes within the range of 2.5–2.7, when ϕ changes from 0 to ϕ_{max}. [19] In the current study, the value of 2.7 was chosen for [η] following ref. [9]. The clear liquid viscosity was extrapolated from the experimental data points of the highest temperature, since no viscosity model could produce reasonable predictions for western coal slag. The average density of spinel, i.e. 3.64 g/cm^3, [17] was chosen as the particle density. The other pertinent parameters used in Veytsman's model are listed in Table 5.

Figure 6 shows the lack of sensitivity to particle size distribution in the Veytsman's model. This is not surprising since the solid fractions encountered in this study are relatively low, i.e. less than 0.2, compared to slurries for which the model was developed. As mentioned earlier, in Veytsman's model, it can be proven mathematically that plastic viscosity is sensitive to ϕ_{max} (or size distribution) when ϕ_{max} is close to ϕ. In this case, the crystal size distribution would have minimal influence on the predicted plastic viscosity. A monodispersed particle size of 22 μm was assumed for the sake of the calculation.

For both models, the solid fraction (ϕ) was obtained by adding the solid phase fractions from Figure 5 and converting to the volume fraction with the calculated density. The case with ZrO_2 dissolution was used in these calculations.

Parameters	Values
[η] – intrinsic viscosity	2.7
Clear Liquid Density (4.19 g/cm^3)	4.19
Particle Density, g/cm^3	3.64
ϕ_0 – close pack ratio	0.637
Particle size (μm)	22
ϕ_{max} – maximum solid loading	0.637
Clear liquid viscosity: η_0 (Pa·s)	$\eta_0 = 5.1837 \times 10^{-6}$ (Pa·s) $\exp\left(\frac{166.09(\text{kJ})}{RT(\text{K})}\right)$

Table 5: Pertinent parameters used in Veytsman's model

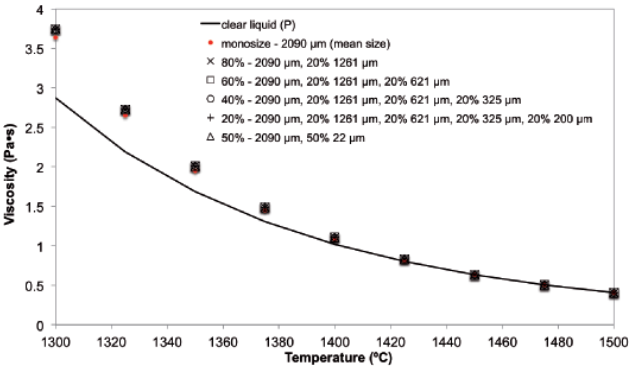

Fig. 6: Sensitivity to the parameters in Veytsman's model.

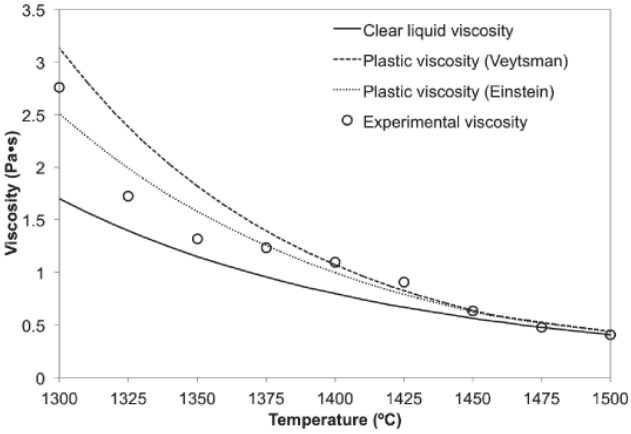

Fig. 7: Predicted viscosity using Veytsman and Einstein Models vs Experiment using solid fraction including zirconia.

Figure 7 shows the experimental points of WC-M2 dataset along with (i) the extrapolated liquid viscosity, and (ii) the resulting prediction from Veytsman – and (iii) Einstein – models. It can be seen that the data is within the error of the experimental data reasonably represented by both models.

Based upon the present results, the values in Table 6 are recommended for use with equations (1) and (2) to predict the plastic viscosity of US western coal slags (excluding ZrO_2).

In order to evaluate the effect on viscosity when the western coal slag is added to the eastern coal slag that only slightly crystallize in viscosity studies, [12] calculations were made for blends of the two, i.e. 10%EC–90%WC, 30%EC–70%WC, 60%EC–40%WC and 90%EC–10%WC (all in mass percentage). The compositions of the blends were calculated using the EC-VS and WC-VS compositions

Temperature range	Recommended parameters and equations	
1773–1757.5 K (1500–1484.5 °C*)	$\eta = 5.1837\times10^{-6}\,(\text{Pa·s})\exp\left(\frac{166.09(\text{kJ})}{RT(\text{K})}\right)$	
Below 1757.5 K (1484.5 °C)	Plastic viscosity, Pa·s (Veytsman)	$\eta=\eta_0\left(1-\frac{\phi}{\phi_{\max}}\right)^{-[\eta]\phi_{\max}}$ $[\eta]=2.7,\ \phi_{\max}=0.637$
	Effective viscosity, Pa·s (Einstein)	$\eta=\eta_0\left(1+\frac{5}{2}\phi\right)$
	Clear liquid viscosity, Pa·s	$=5.1837\times10\ \ (\text{Pa·s})\exp\left(\frac{166.09(\text{kJ})}{RT(\text{K})}\right)$
	Volume fraction of solids, $\phi<0.2$, T in K	$\phi=f(T)=2\times10^{-9}T^3+8\times10^{-6}T^2-0.0118T+6.5315$

* 1757.5 K (1484.5 °C) is the transition temperature when first crystals precipitate.

Table 6: Recommended parameters and equations for predicting plastic viscosity of US western coal slags (excluding ZrO_2) in the temperature range of 1773–1573 K (1500–1300 °C)

shown in Table 2, and a solid phase mass fraction was calculated by FactSage for each blend, then converted to the volume fraction by K.C. Mills method [16] (Figure 8a). Up to 14 wt% of anorthite was noted in FactSage calculations for 90 to 60 mass% EC–WC mixtures. The formation of anorthite was neglected here as it was not observed in the present experiment within the time studied. The clear liquid viscosities were predicted with FactSage for each chemistry blend. The same $[\eta]$ and $\phi_{\max}$ values were used in Veytsman's model for calculating the plastic viscosities shown in Figure 8b. The viscosity of 100 mass% eastern coal slag was evaluated experimentally in an earlier study, [12] which is also shown in Figure 8b. It can be seen that the plastic viscosity calculated with Veytsman's model for the 100 mass% eastern coal slag agrees rather well the experimental value.

FactSage calculations indicated spinel would form in slags with 70%EC–30%WC through 100%WC, while mullite was only noted for EC-rich slags (100%EC up to 90%EC–10%WC). Note anorthite was again assumed to be negligible and not included in calculations shown in Figure 8. A discussion of the formation kinetics of anorthite is beyond the scope of this study. For all blend chemistries, a positive deviation was noted below the transition temperature at which crystals started to precipitate. This transition temperature varied with slag blend compositions, see Figure 9. According to FactSage, the liquidus temperature of 100%WC is 1757.5 K (1484.5 °C), which decreases down to 1604.4 K (1331.4 °C) at 70%EC–30%WC, with increasing EC%. The liquidus temperature then increased at higher EC% to 1686.6 K (1413.6 °C) for 100%EC. This trend is correlated to the types of solids formed in the slags, i.e. spinel or mullite. A general trend that the viscosity decreases at higher WC% at any temperatures studied here may be related to an increase in basicity (CaO/SiO_2) for acidic slags.

4 Conclusions

The viscosity of the synthetic slags with chemistry resembling the molten ash of coal from the western United States was measured with a rotating-bob viscometer. It was found that the viscosity was significantly lower than the eastern coal, and that its viscosity could not be described by a single Arrhenius type function. Significant crystallization of $(Mg,Fe)Al_2O_4$-based spinel was attributed to be the cause. Spinel crystals precipitated at temperatures below 1757.5 K (1484.5 °C), and the results suggest that their growth was rapid to be close to the solid fraction predicted by phase equilibrium calculations at temperatures above 1573 K (1300 °C). The viscosity could be described by a clear liquid viscosity of $\eta_0 = 5.1837\times10^{-6}\,(\text{Pa·s})\exp\left(\frac{166.09(\text{kJ})}{RT(\text{K})}\right)$ in the temperature range above 1757.5 K, and by a plastic viscosity model given by $\eta=\eta_0\left(1-\frac{\phi}{\phi_{\max}}\right)^{-[\eta]\phi_{\max}}$ using a volume fraction solid obtained from FactSage below that temperature.

Acknowledgements

This technical effort was performed in support of the National Energy Technology Laboratory's ongoing research in development of coal gasification under the RES contract DE-FE0004000.

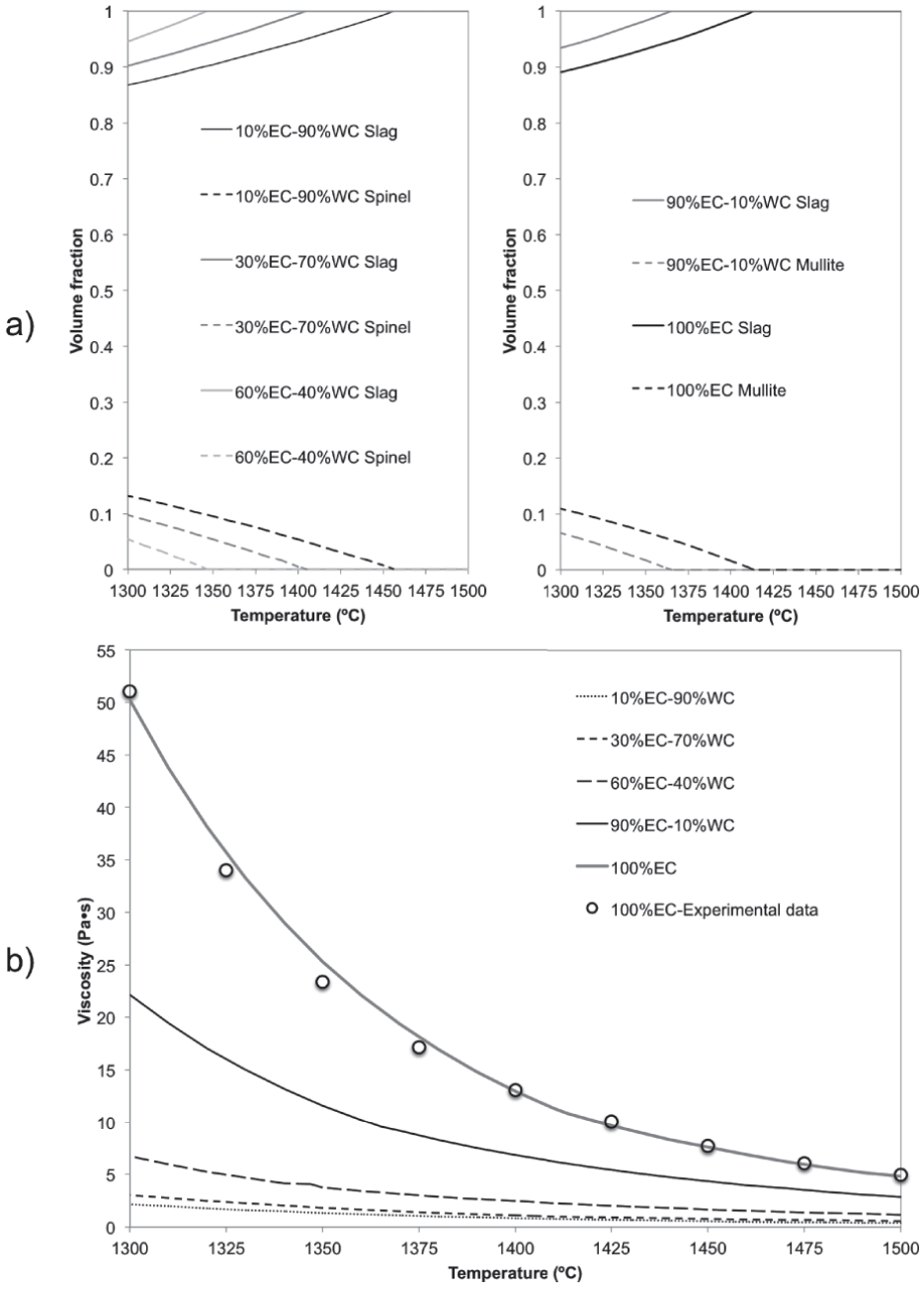

Fig. 8: (a) The solid volume fraction in eastern and western coal blends (mass%) on an ash basis (without considering ZrO_2.) calculated with FactSage. (b) Predicted viscosity of slag blends with Veytsman model and using solids fractions in figure 8a.

Disclaimer: "This report was prepared as an account of work sponsored by an agency of the United States Government. Neither the United States Government nor any agency thereof, nor any of their employees, makes any warranty, express or implied, or assumes any legal liability or responsibility for the accuracy, completeness, or usefulness of any information, apparatus, product, or process disclosed, or represents that its use would not infringe privately owned rights. Reference herein to any specific commercial product, process, or service by trade name, trademark, manufacturer, or otherwise does not necessarily constitute or imply its endorsement, recommendation, or favoring by the United States Government or any agency thereof. The views and opinions of authors expressed herein do not necessarily state or reflect those of the United States Government or any agency thereof."

Received: May 16, 2012. Accepted: July 12, 2012.

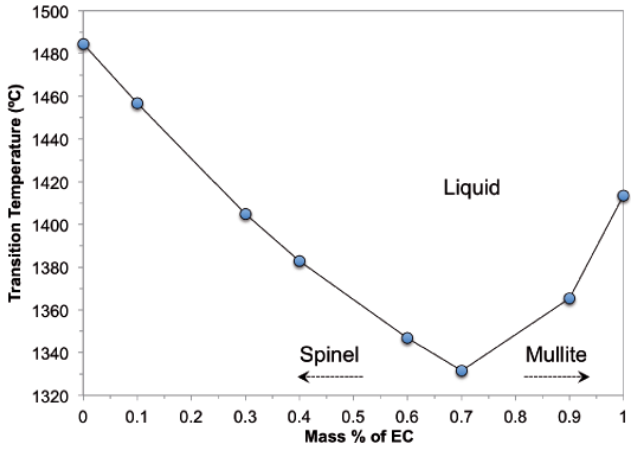

Fig. 9: The transition temperatures of the EC and WC blends as calculated using FactSage.

References

[1] J.P. Bennett, K. Kwong, C. Powell, R. Krabbe, H. Thomas, and A. Petty. Low Chrome/Chrome Free Refractories for Slagging Gasifiers. Research Report DOE/NETL-IR-2006-119, 2006, p. 200–206.

[2] K.S. Vorres, Energy & Fuels, 4,(5), 420–426 (1990).

[3] G.J. Browning, G.W. Bryant, H.J. Hurst, J.A. Lucas, T.F. Wall. Energy & Fuels, 17,(3), 731–737(2003).

[4] D.P. Kalmanovitch, M. Frank. In Engineering Foundation Conference on Mineral Matter and Ash Deposition from Coal, United Engineering Trustees Inc., Santa Barbara, CA, 1988.

[5] A. Kondratiev and E. Jak. *Met. Trans. B*, **32B**, 1015–1025(2001).

[6] G. Urbain, F. Cambier, M. Deletter, M.R. Anseau. *Trans. J. Br. Ceram. Soc.*, **80**, 139–141(1981).

[7] C.W. Bale, A.D. Pelton, and W.T. Thompson. Facility for the Analysis of Chemical Thermodynamics. Ecole Ploytechnique, Montreal, http://www.factsage.com, 2000.

[8] J. Happel and H. Brenner, *Chapter 9 in Low Reynolds Number Hydrodynamics with Special Applications to Particular Media 2nd Ed*, Noordhoff International Publishing, Leyden, Netherlands, (1973), pp. 431–441.

[9] B. Veytsman, J. Morrison, A. Scaroni and P. Painter, *Energy & Fuels*, **12**, 1031–1039(1998).

[10] W.A. Selvig, F.H. Gibson, *Bureau of Mines Bulletin 567*, United States Government Printing Office, Washington, 1956.

[11] K.S. Vorres, "Users Handbook For The Argonne Premium Coal Sample Program", Argonne National Laboratory, http://web.anl.gov/PCS/report/part2.html

[12] J. Zhu, T.K. Kaneko, H. Mu, J.P. Bennett and S. Sridhar, *Proceedings of the Ninth International Conference on Molten Slags, Fluxes and Salts*, May 27–30, 2012, Beijing, China.

[13] J. Nakano, S. Sridhar, T. Moss, J.P. Bennett, K-S. Kwong, *Energy & Fuels*, **23**, 4723–4733(2009).

[14] C. Orrling, S. Sridhar, A.W. Cramb, *High Temp. Mater. Processes*, **20**,(3–4), 195–199(2001).

[15] S. Sridhar, A.W. Cramb, *Metall. Mater. Trans. B*, **31B**,(2), 406–411(2000).

[16] K.C. Mills and B.J. Keene, *Intl. Materials Review*, **32**, 1–120(1987).

[17] http://webmineral.com/data/Spinel.shtml

[18] http://en.wikipedia.org/wiki/ZrO2

[19] I.M. Krieger, *Adv. Colloid Interface Sci.*, **3**, 111–136(1972).